# Macromechanics and polycaprolactone fiber organization drive macrophage polarization and regulate inflammatory activation of tendon in vitro and in vivo

**Journal Article**

**Author(s):**
Schoenenberger, Angelina D.; Tempfer, Herbert; Lehner, Christine; Egloff, Jasmin; Mauracher, Marita; Bird, Anna; Widmer, Jonas; Maniura-Weber, Katharina; Fucentese, Sandro F.; Traweger, Andreas; Silvan, Unai; Snedeker, Jess Gerrit

**Publication date:**
2020-08

**Permanent link:**
https://doi.org/10.3929/ethz-b-000411494



**Originally published in:**
Biomaterials 249, https://doi.org/10.1016/j.biomaterials.2020.120034

Biomaterials 249 (2020) 120034

Contents lists available at ScienceDirect

Biomaterials

journal homepage: www.elsevier.com/locate/biomaterials

# Macromechanics and polycaprolactone fiber organization drive macrophage polarization and regulate inflammatory activation of tendon *in vitro* and *in vivo*

Angelina D. Schoenenberger[a,b], Herbert Tempfer[c,d], Christine Lehner[c,d], Jasmin Egloff[a,b], Marita Mauracher[a,b], Anna Bird[a,b], Jonas Widmer[a,b], Katharina Maniura-Weber[e], Sandro F. Fucentese[a], Andreas Traweger[c,d], Unai Silvan[a,b], Jess G. Snedeker[a,b,**]

[a] *Department of Orthopedics, Balgrist Hospital, University of Zurich, Zurich, Switzerland*
[b] *Institute for Biomechanics, ETH Zurich, Zurich, Switzerland*
[c] *Institute of Tendon and Bone Regeneration, Paracelsus Medical University - Spinal Cord Injury & Tissue Regeneration Center Salzburg, Salzburg, Austria*
[d] *Austrian Cluster for Tissue Regeneration, Vienna, Austria*
[e] *Biointerfaces, Empa, Swiss Federal Laboratories for Material Science and Technology, St. Gallen, Switzerland*

ARTICLE INFO

*Keywords:*
Topography
Nanofibers
Inflammation
Macrophage
Mechanobiology
Tendon

ABSTRACT

Appropriate macrophage response to an implanted biomaterial is crucial for successful tissue healing outcomes. In this work we investigated how intrinsic topological cues from electrospun biomaterials and extrinsic mechanical loads cooperate to guide macrophage activation and macrophage-tendon fibroblast cross-talk. We performed a series of *in vitro* and *in vivo* experiments using aligned or randomly oriented polycaprolactone nanofiber substrates in both mechanically loaded and unloaded conditions. Across all experiments a disorganized biomaterial fiber topography was alone sufficient to promote a pro-inflammatory signature in macrophages, tendon fibroblasts, and tendon tissue. Extrinsic mechanical loading was found to strongly regulate the character of this signature by reducing pro-inflammatory markers both *in vitro* and *in vivo*. We observed that macrophages generally displayed a stronger response to biophysical cues than tendon fibroblasts, with dominant effects of cross-talk between these cell types observed in mechanical co-culture models. Collectively our data suggest that macrophages play a potentially important role as mechanosensory cells in tendon repair, and provide insight into how biological response might be therapeutically modulated by rational biomaterial designs that address the biomechanical niche of recruited cells.

## 1. Introduction

The use of 'mechanical augmentation' with biomaterial patches that increase strength of surgically repaired soft tissues has emerged as a major clinical advance in orthopedic medicine, with increasing use of a wide range of natural or synthetic patches [1–4]. While natural extracellular matrix (ECM)-derived scaffolds, such as collagen patches, provide strong cues for cell infiltration, their degradation rate is rapid and the mechanical support they offer is therefore limited [3,5]. On the other hand, biodegradable synthetic polymers offer tunable degradation characteristics to provide initial mechanical support during the critical tissue regeneration phase [2,6]. In particular, electrospun fiber scaffolds can be designed to resemble native tissue ECM, for instance mimicking the highly aligned collagen fiber matrix that characterizes healthy tendon [7–10]. Among candidate patch materials, polycaprolactone (PCL) nanofiber scaffolds are synthetic, degradable and biomimetic constructs that offer good biocompatibility, slow degradation rates and 'tunable' mechanical properties [11–14]. Due to their capacity to promote tissue healing by simultaneously providing biological cues and mechanical support, clinical use of such scaffolds is growing [2].

Beyond the choice of the bulk biomaterial itself, a wide range of design parameters can be varied to exert control over host tissue response. How biomaterial substrate mechanics and biochemistry interact to guide cell behavior has emerged as an important research topic with broad implications to biomaterial design [15–17]. Specifically for tendon repair, an aligned micro- or nanofiber structure is now understood to be a highly instructive biophysical cue that can direct tendon

* Corresponding author. Balgrist Campus, Lengghalde 5, 8008, Zurich, Switzerland.
*E-mail address:* snedeker@access.uzh.ch (J.G. Snedeker).

https://doi.org/10.1016/j.biomaterials.2020.120034
Received 30 March 2019; Received in revised form 4 April 2020; Accepted 5 April 2020
Available online 11 April 2020

specific lineage differentiation [18–25]. Our own work has shown that deviations from aligned biomaterial surface structures may play a potentially important role in predisposing inflammatory response of attached tendon fibroblasts [26]. However tendon fibroblast-surface interactions are just one aspect of biomaterial host interaction that is likely to be further affected by presence of progenitor and immune cells, as well as the mechanical forces that pervade implanted orthopedic biomaterials [27–30].

While resident tissue fibroblasts and their progenitors have been identified as sensitive to intrinsic mechanical and biophysical cues from a biomaterial, considerably less is known about immune cell response to extrinsic mechanical stretch [31]. Immune cells, particularly macrophages, are among the first cells to respond to implanted biomaterials. Their initial interaction and, more specifically, their polarization from an initial pro-inflammatory (M1-like) phenotype towards a reparative (M2-like) phenotype, is crucial for successful tissue-biomaterial integration [32]. Macrophages have the ability to polarize into a broad spectrum of phenotypes and the high degree of plasticity allows them a shift in the polarization state from M1 to M2 [33–35]. Therefore, 'immuno-modulatory' design characteristics of regenerative biomaterials, which induce favorable immune response upon implantation, may be a powerful tool to achieve improved healing outcomes [36,37].

In this work we present a range of *in vitro* and *in vivo* studies to characterize the effects of mechanical cues presented to macrophages and/or human tendon fibroblasts (hTFs) from electrospun PCL scaffolds mimicking those used in surgical repairs of torn tendons. The *in vitro* studies model the first interaction of macrophages and hTFs within a mechanically challenged biomaterial, allowing study in a tightly controlled environment that includes the impact of mechanical and topographical cues on macrophage activation. Using this system, we sought to clarify how macrophage inflammatory response may be regulated by mechanical loads and potentially be modulated for a positive tendon healing outcome. These responses were then verified *in vivo*, using the same electrospun scaffolds implanted in rat Achilles tendons to investigate how biophysical cues from aligned and random scaffolds affect early healing response (inflammation and cell invasion). The impact of *in vivo* mechanical loads was investigated by comparing a normal mechanical loading against a Botox-treated group.

These studies were broadly aimed at characterizing how topographical cues and mechanical load interact to potentially drive macrophage polarization. The work was motivated by the fact that the PCL fiber orientation can predispose the inflammatory response of hTFs [26], and the plausibility that similar regulation of immune cells may meaningfully influence the initial healing phase after surgery. We therefore specifically investigated and characterized the response of hTFs to mechanical loading in direct and indirect contact with macrophages.

Across all studies, our results indicate that disorganized biomaterial topographies (mimetic of a disorganized collagen matrix) alone are sufficient to provoke release of pro-inflammatory cytokines by macrophages. *In vitro* experiments on tendon fibroblasts without contact to macrophages (i.e. mechanical monoculture) showed that this pro-inflammatory activation was promoted by dynamic mechanical loading (7% strain, a level mimicking anabolic mechanical stimulus). For instance, when tendon cells were incubated in macrophage conditioned medium generated by mechanical stimulation of naïve macrophages in monoculture, nuclear translocation of the p65 subunit of the NFκB complex in human tendon fibroblasts was significantly increased. Surprisingly, direct mechanical co-culture of M0 macrophages and hTFs muted both tendon and macrophage responses to loading in comparison to monoculture, highlighting a potentially central importance of direct cell-cell communication in promoting M2-like macrophage polarization. These *in vitro* findings were robustly confirmed by the *in vivo* experiments. Impressively, the sensitivity of macrophages to substrate topography and mechanical stimulus was more profound than that of the tendon fibroblasts, suggesting a currently hitherto unappreciated but perhaps central role for macrophages as mechano-regulators of tendon repair.

## 2. Results

Beyond mechanical reinforcement of repaired tissues, regenerative biomaterials provide biophysical cues that affect the response of immune and tissue-resident cells [38–40]. Classically, surface micro- and nano-topography and chemical composition have been considered central to this response, and these properties have been consequently considered in biomaterial design [40]. However, the potential interactions between resident fibroblasts and macrophages in the context of biomaterial topography and mechanical forces are currently undescribed. We therefore performed a series of experiments on tendon cells, macrophages, and synthetic biomaterials relevant to current clinical practice, using an *in vitro* model system to study the effect of topography and strain deformations on macrophages and human tendon fibroblasts (hTFs) in both indirect and direct cell-cell contact [26,41].

### 2.1. Disorganized substrate topography initiates macrophage polarization in vitro

To investigate the potential shift in polarization of M0 macrophages cultured on aligned and random electrospun polycaprolactone surfaces with mean fiber diameter of 700 nm [40], we cultured these cells on the structured surfaces for 24 h and examined their morphology and polarization profile. Consistent with previous studies [40,42] scanning electron microscopy (SEM) images revealed marked morphological differences between experimental conditions, with macrophages being substantially more spread on randomly oriented topographies than on aligned ones (Fig. 1A). Immunostaining revealed a heterogeneous expression of CCR7 (CD197, M1-marker) and MRC1 (CD206, M2-marker) on both substrates (Supplementary Fig. S6). A heterogeneous gene expression with no obvious difference between the substrate topographies was also seen in quantitative PCR (qPCR) for these markers (Fig. 1B, left panel). However, flow cytometry analysis revealed that M0 macrophages cultures on substrates with random fiber orientation demonstrated a moderate but significantly higher percentage of $CCR7^+$ positive cells indicating a polarization shift towards a pro-inflammatory (M1-like) phenotype (Fig. 1C). Furthermore, the cell population positive for $MRC1^+$ (M2 marker) was similar for both substrate topographies. The expression level of *IL1B* appeared significantly increased in cells cultured on randomly oriented substrates when compared to those on aligned ones, whereas *TNF* and *TGFB1* levels remained unchanged (Fig. 1B, right panel). Analysis of macrophage-conditioned media by U-PLEX ELISA revealed significant differences in secretion of the pro-inflammatory cytokine TNF on randomly oriented substrate topographies (Fig. 1D), with a non-significant difference in IL1β that was nonetheless in agreement with gene expression level analysis being higher in cells cultured on random substrates.

### 2.2. Dynamic mechanical loading drives macrophage polarization toward a pro-inflammatory phenotype in vitro

Testing the impact of load on their polarization, M0 macrophages were exposed to either static (1% constant baseline strain) or dynamic loading (7% cyclic strain at 1 Hz), consisting of 8 h conditioning, followed by a 16 h resting period. Independently of substrate topography, dynamic loading caused a significant upregulation of *CCR7* (M1-marker) indicating a polarization towards a pro-inflammatory phenotype (Fig. 2A). Conversely, expression of *MRC1* (M2-marker) was not affected by either topography or loading (Fig. 2B). The trend for the polarization towards the pro-inflammatory phenotype observed in gene expression was further confirmed with flow cytometry by a higher percentage of $CCR7^+$ cells (Fig. 2C). Although differences did not reach

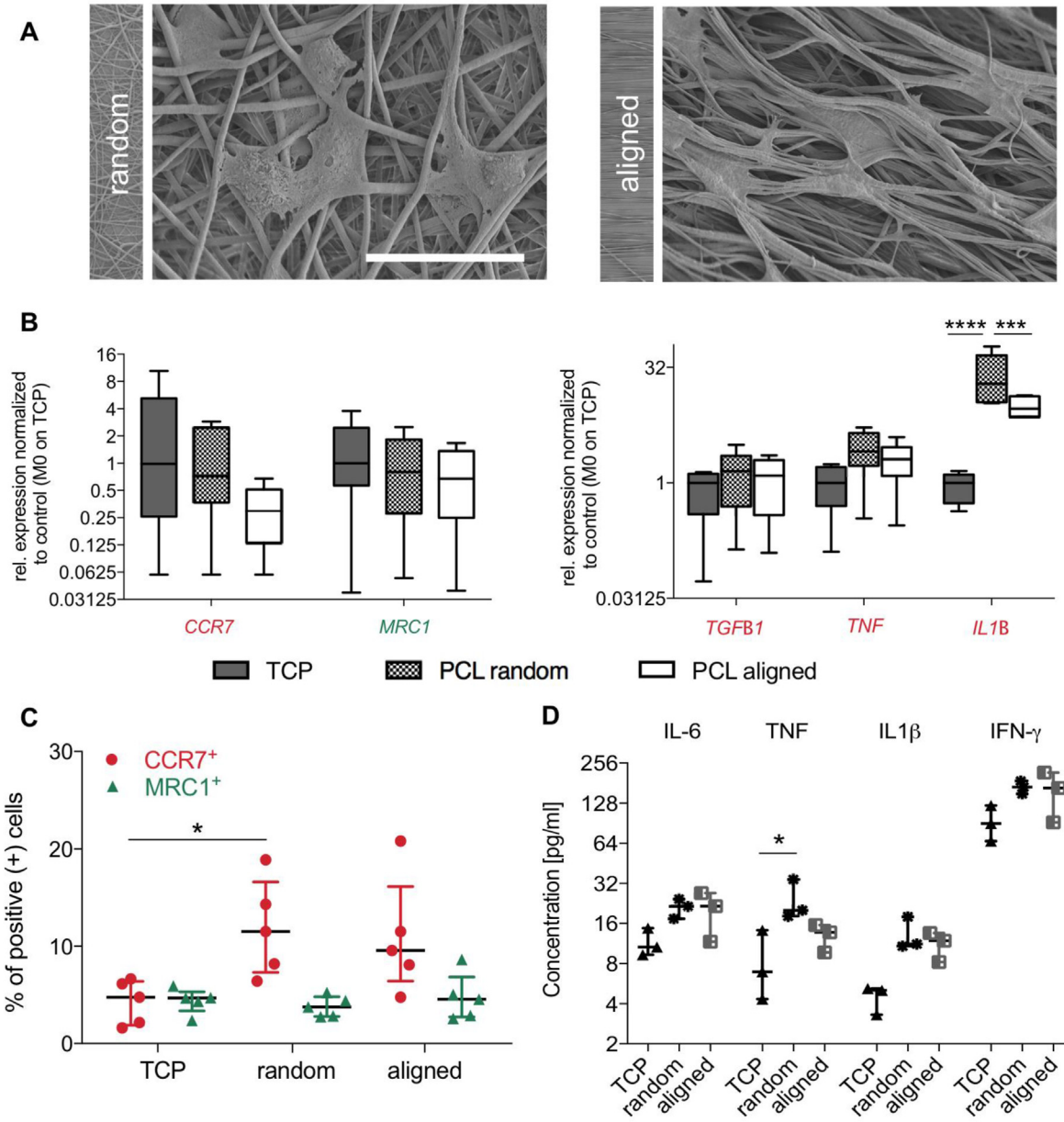


**Fig. 1. Randomly oriented substrates tend macrophage polarization toward an increased pro-inflammatory phenotype in vitro.** (A) SEM images showed morphological differences between macrophages attached to random (left panel) and aligned (right panel) PCL substrates with mean fiber diameter of 700 nm, with more elongated cells on aligned substrates. (B) Gene expression levels of CCR7 (M1-like) and MRC1 (M2-like) were similar in M0 macrophages cultured on random (checkerboard box) and aligned (white box) substrates. In cells cultured on the randomly oriented fibers, significantly increased expression of IL1B was detected, whereas TNF and TGFB1 expression levels remained unchanged. (C) Flow cytometry analysis revealed the polarization of M0 macrophages towards the pro-inflammatory ($CCR7^+$) phenotype when cultured on the random substrates. The evaluation was performed by measuring the percentage of CCR7 (red dots) and MRC1 (green triangles) positive cells in M0 macrophages cultured on random and aligned PCL nanofiber substrates. (D) Cytokine secretion in macrophages exposed to the different topography cues displayed a significantly increased protein release of the pro-inflammatory cytokine TNF in cells cultured on random substrates. Data are presented as the median of n = 6 (B), 5 (C), 3 (D) with the interquartile range and are considered significantly different when *P ≤ 0.05. Statistical analysis was performed by a two-way ANOVA with Tukey's multiple comparisons test to assess the statistical difference on the gene expression level between the groups (B). Further, the Kruskal Wallis non-parametric ANOVA with Dunn's post-test was performed comparing every treatment with its corresponding control (M0 on TCP) (C, D) (*P ≤ 0.05, ***P ≤ 0.001, ****P ≤ 0.0001). Scale bar represents 50 μm (magnification). (For interpretation of the references to colour in this figure legend, the reader is referred to the Web version of this article.)

significance, changes in the gene expression levels for pro-inflammatory cytokines *IL1B*, *TNF* and *TGFB1* were observed (Fig. 2D–F).

### 2.3. Secreted factors from mechanically challenged macrophages induce NFκB pathway activation in statically cultured tendon fibroblasts in vitro

Having observed a more pro-inflammatory activation potential of random scaffolds on macrophages, we then analyzed the response of hTFs stimulated with their released factors. Briefly, conditioned medium (CM) was collected after mechanical stimulation of macrophages and added to hTFs seeded on aligned substrates. Analysis of the culture medium by multiplex ELISA revealed a high degree of variability in cytokine secretion, with non-significant differences between the conditions (Fig. 3A). These observations were supported by analysis of nuclear translocation of NFκB-p65 in hTFs 30 min after stimulation by macrophage conditioned medium as well as gene expression at 24 h

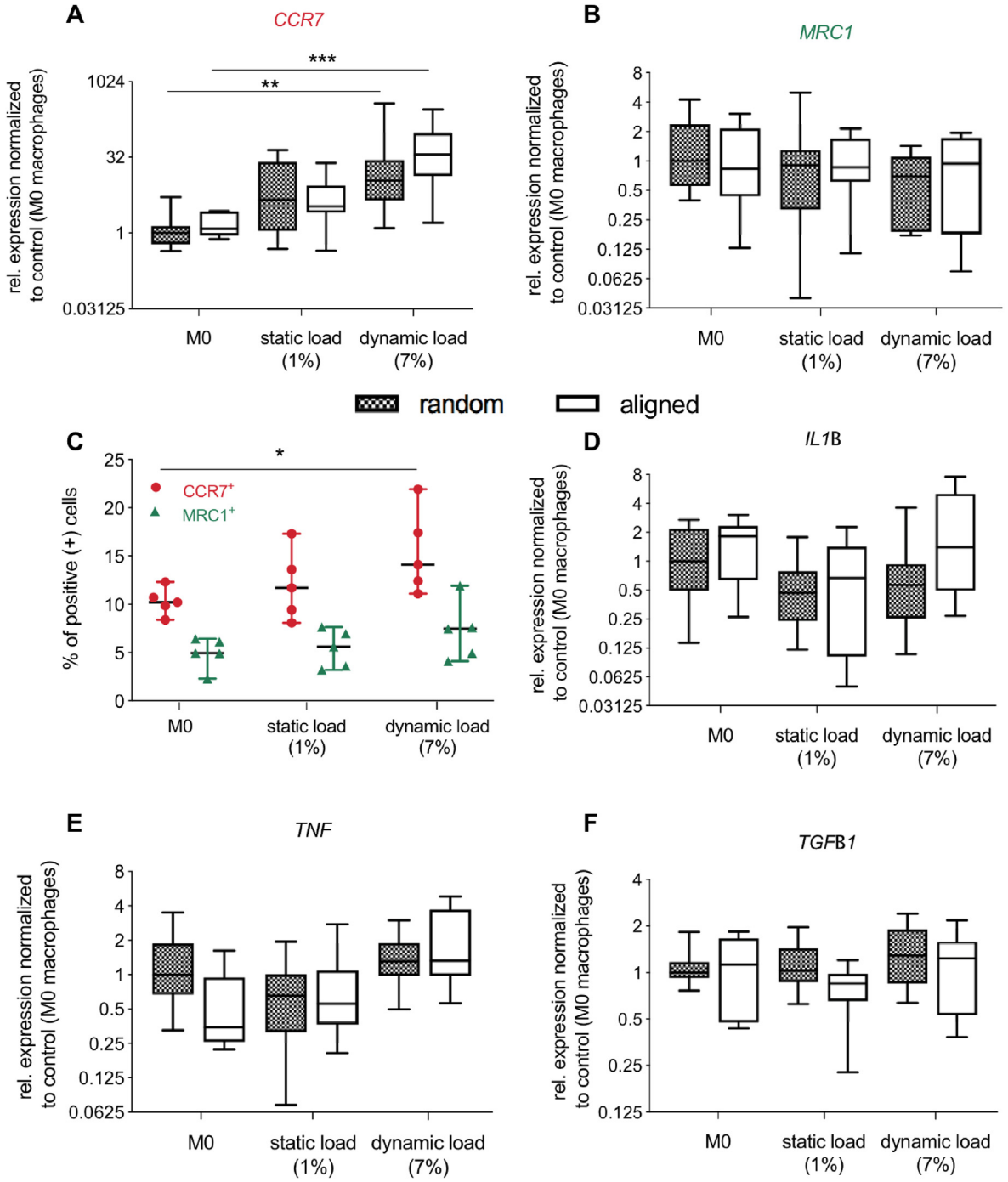


**Fig. 2. Dynamic loading of M0 macrophages induces a polarization shift towards the pro-inflammatory M1-like phenotype in vitro.** (A,B) Mechanical loading upregulates CCR7 (M1 marker) expression in M0 macrophages. A significant increase in CCR7 was found due to dynamic loading, whereas MRC1 gene expression remained unaltered (n = 9). (C) The percentage of CCR7 positive cells reveal a polarization shift in the dynamically loaded cell population compared to the unloaded control (M0 on random substrates) (n = 6). (D–F) In addition, gene expression levels of the inflammatory cytokines IL1B, TNF and TGFB1 were measured in response to dynamic loading compared to the static loading condition. Results were normalized to M0 macrophages on random, unloaded substrates by dividing through its median (n = 9). Statistical analysis was performed using Kruskal Wallis non-parametric one-way ANOVA with Dunn's post-test comparing every treatment with its corresponding control (M0 on PCL random or aligned) (*P ≤ 0.05, **P ≤ 0.01, ***P ≤ 0.001).

(Fig. 3B, C and D). Here, the factors secreted by dynamically loaded macrophages provoked a significant increase in p65 nuclear translocation in hTFs than the supernatant of statically loaded macrophages.

### 2.4. NFκB pathway activation by IL1B stimulation is dampened in mechanically loaded human tendon fibroblasts in vitro

The response of human tendon fibroblasts (hTFs) to the scaffolds was analyzed, specifically the impact of the previously described loading protocols (static and dynamic) on the response of hTFs – independently of macrophage presence in the culture system. An adaptation of the nucelar shape was found in response to applied static and dynamic loads (Fig. 4A). The calculated aspect ratio indicated a significant increased nuclear elongation in the cells cultured on both constructs due to static load, being further increased due to dynamic load in the cells cultured on the aligned constructs. Direct mechanical

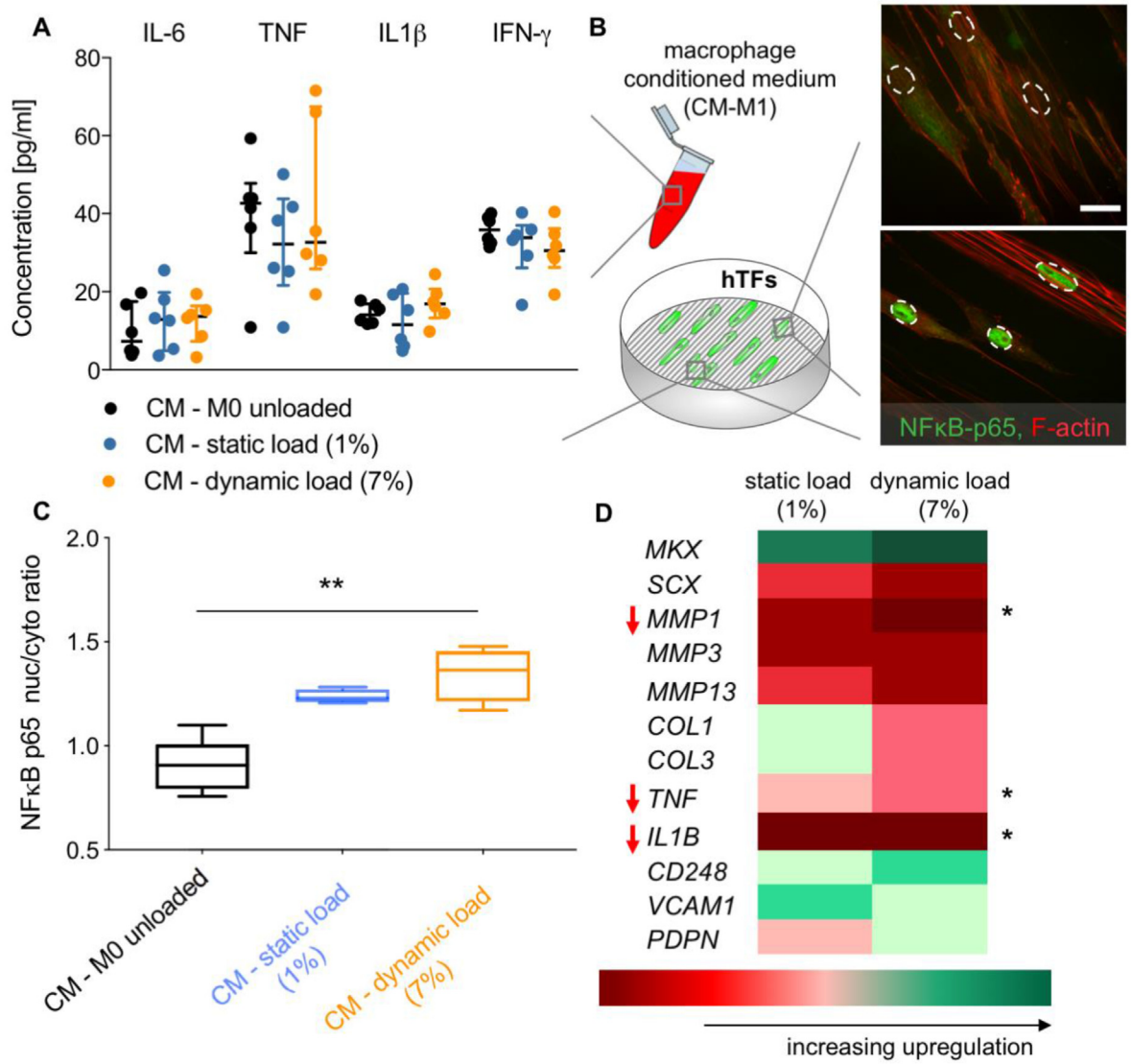


**Fig. 3. Immunoresponse of hTFs stimulated with macrophage conditioned medium (CM) in vitro.** (A) Cytokine secretion in mechanically conditioned macrophages was measured in the supernatant using a multiplex ELISA. Levels of IL-6, TNF, IL1β and IFN-γ were measured in the supernatant of mechanically loaded (1% and 7% strain) and unloaded macrophages (n = 6). (B) hTFs seeded on aligned substrates stained for F-actin (red) and NFκB-p65 (green) stimulated with macrophage conditioned medium of the pro-inflammatory macrophages (CM-M1) (the dotted line indicates the location of the nuclei). (C) Immunostaining against p65 revealed significantly increased nuclear p65 in hTFs stimulated with CM from dynamically loaded macrophages. Medium conditioned by unloaded M0 macrophages cultured on random substrates was used as control (n = 4). (D) Gene expression analysis reveals lower expression of MMP1 in hTFs stimulated with CM from mechanically loaded macrophages. Tenogenic gene expression and fibroblast activation markers were not significantly altered in hTFs stimulated with CM. In addition, significantly smaller expression levels of inflammatory cytokines TNF and IL1B were found in hTFs exposed to medium from mechanically loaded macrophages (n = 6). Statistical analysis was performed using Kruskal Wallis non-parametric ANOVA with Dunn's post-test comparing every treatment with its corresponding control (CM of M0 unloaded) (*P ≤ 0.05, **P ≤ 0.001). Scale bar represents 20 μm. (For interpretation of the references to colour in this figure legend, the reader is referred to the Web version of this article.)

stimulation of human tendon fibroblasts induced translocation of p65 to the nucleus, indicating activation of the NFκB pathway (Fig. 4B). This observed mechano-activation was more pronounced in cells on the random topology constructs. In seeming contrast to increased p65 nuclear presence in mechanically stimulated hTFs, mechanical load was found to be protective against the dramatic NFκB pathway activation caused by IL1B (Fig. 4C).

### *2.5. Direct co-culture of M0 and hTFs activates the NFκB pathway with diminished expression of M1-like markers, and mechanically induced increase of M2-like markers in vitro*

Cross-talk of macrophages and hTFs was analyzed in a direct co-culture study (Fig. 5A). Both cell types were cultured on aligned PCL scaffolds in a 4:1 (M0:hTF) ratio for 24 h before applying the mechanical loading protocol lasting another 24 h. Nuclear translocation of NFκB-p65 in hTFs cultured in direct co-culture with macrophages was significantly increased compared to hTFs cultured alone. Interestingly, dynamic load in direct co-culture samples did not promote further p65 nuclear translocation (Fig. 5B). Next, we performed flow cytometry analysis using CD90 as hTF marker and CD14 for monocyte detection (Fig. 5C). Subsequently, $CD14^+/CD90^-$ cells were further gated for $CCR7^+$ (M1-type macrophages) and $MRC1^+$ (M2-type macrophages) (Fig. 5D). The results indicate that direct co-culture led to a reduction in the $CCR7^+$ (M1-marker) from 4.5% to 4.32% cell population and additional loading with 7% strain led to an increase in the $MRC1^+$ (M2-marker) cell population from 2.14% to 4.7%.

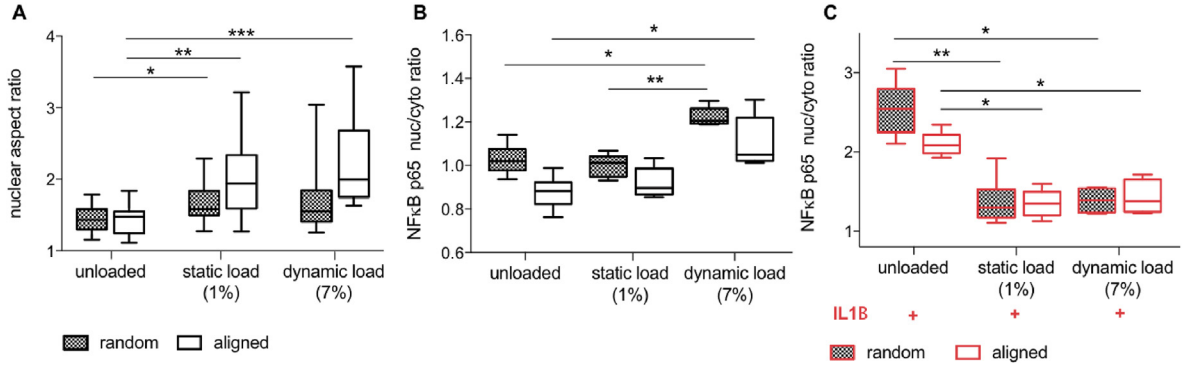


**Fig. 4. Mechanical loading protects against NFκB activation by IL1B in vitro.** (A) Quantification of nuclear aspect ratio indicated a significantly increased elongation of the nuclear shape in response to load, being more marked in cells cultured on the aligned substrates (white box) (n = 3). (B) Dynamic loading of hTFs results in increased nuclear p65 presence. This effect was more pronounced in cells seeded on random (checkerboard box) than on aligned (white box) substrate (n = 6). (C) Pro-inflammatory stimulation with IL1B following mechanical stimulation significantly reduced p65 subunit translocation (n = 6). Statistical analysis was performed using Kruskal Wallis non-parametric ANOVA with Dunn's post-test comparing every treatment and with its corresponding control (M0 on PCL random or aligned, unloaded) (*P ≤ 0.05, **P ≤ 0.01, ***P ≤ 0.001).

### *2.6. Topographical and mechanical cues drive the immune response in vivo, with mechanical loading and scaffold fiber alignment suppressing inflammatory activation*

Using an *in vivo* rat model, we then studied the immune response to aligned and randomly oriented PCL scaffolds [43]. For that we implanted 4 $mm^2$ random and aligned scaffolds within the core tendon tissue of the Achilles tendons of rats. The regulation of host-biomaterial interaction by extrinsic muscle forces to the tendon was studied using Botulinum toxin (Botox) treatment. Nuclear staining of longitudinal cryosections of the scaffolds 7 days after surgery revealed that in all experimental conditions host cells densely populated both scaffold types (Fig. 6A–B), with organization of the newly formed tissue within and around the scaffold being qualitatively more disorganized in randomly oriented scaffolds. Semi-quantitative analysis of immunohistochemistry sections indicated a tendency toward more CD68 positive cells located around and within the randomly oriented scaffold with the lowest number of $CD68^+$ cells in aligned scaffolds under mechanical load (Fig. 6C).

Neo-tissue formation and immunofluorescent quantification of IL-1β expression within the implanted scaffolds revealed clear sensitivity to PCL fiber orientation as well as extrinsic mechanical load ($p < 0.05$; Fig. 7). The IL-1β expression signature was strongly and significantly elevated with inhibition of muscle loads. While immunofluorescence signal of IL-6 was detectable in all experimental conditions (Fig. 7D), it was lowest in aligned scaffolds, particularly aligned scaffolds in mechanically underloaded conditions.

## 3. Discussion

Synthetic biodegradable patches employed for surgical repair of soft tissues require a certain mechanical elasticity, as the materials themselves can be subjected to large deformations. The deformation of a biomaterial to applied forces has been shown to influence the phenotypic profile of attached macrophages [44–46] but the potential impact this may have on the host tissue healing is poorly understood and largely uninvestigated [37]. Animal experiments have recently revealed that microarchitectural design factors [47] such as fiber alignment [20] can affect the quality of tendon neo-tissue formation. In the present work, we aimed to clarify how mechano-regulation of macrophages may be co-regulated by substrate topography, and further investigate cross-talk with tendon fibroblasts in the context of surgical patches for the augmented repair of torn rotator cuff tendons.

The host response to an implanted synthetic biomaterial heavily depends on cross-talk between tissue resident fibroblasts and cells of the immune system [30,40,48] While this response is likely to be central to eventual clinical outcome, the involved cellular interactions are complex and challenging to study [48]. In the present work, we introduce a range of simplified *in vitro* models that offer to help unwind some of this complexity, allowing focused investigation on the effect of topographical cues and mechanical loading on primary human tendon fibroblasts and a cell line model of human macrophages. We used these models to study both their individual and cooperative behavior. We specifically focused on inflammatory activation of tendon fibroblasts and polarization of macrophages – both potentially important drivers of host tissue response to a biomaterial [40]. The clinical motivation for the present study was to better understand biomaterial-fibroblast-macrophage interactions in the scope of synthetic biomaterial patches employed for tendon repair surgery, and how the design and/or deployment of a patch may affect outcome.

It has been shown that upon surgical implantation cellular response and macrophage polarization can be mediated by biomaterial topography cues through the control of cell shape [49]. In fact, it has been reported that during the first hours after their initial contact with a biomaterial, topographical cues can override effects of the underlying surface chemistry [40]. Interestingly, nanofiber cues compared to micro-fiber cues have particular potential to alter fibroblast response from repair to healing [25]. Furthermore, it has been demonstrated that different inflammatory responses were elicited depending on biomaterial grating patterns or electrospun fibers of different thickness and compositions [50–52]. While the description of the underlying links between inflammatory mechanisms and tendon homeostasis is thus crucial to understand the factors that drive tissue repair quality [53], these links have been under-investigated. We performed a series of targeted experiments to address this knowledge gap.

In a first step, we mechanically characterized the tensile properties of two electrospun polycaprolactone substrates similar fiber diameter distributions with but highly variant fiber orientations. Both revealed similar stress-strain characteristics (Supplementary Fig. S1). Next, we analyzed the baseline response of M0 macrophages as a function of biomaterial topography, using short-term (24 h) exposure to random and aligned polycaprolactone (PCL) nanofiber substrates. Analysis of cell morphology revealed substantially more elongated shapes of the M0 macrophages on aligned substrates. Such cell shapes have been previously associated with M2-like polarization [42]. Our results support these studies demonstrating that disorganized nanofiber topography alone is able to initiate polarization of M0 macrophages towards a pro-inflammatory phenotype. In addition, we observed that M0 macrophages cultured on randomly structured substrates exhibited significantly increased levels of the pro-inflammatory cytokines *IL1B* at

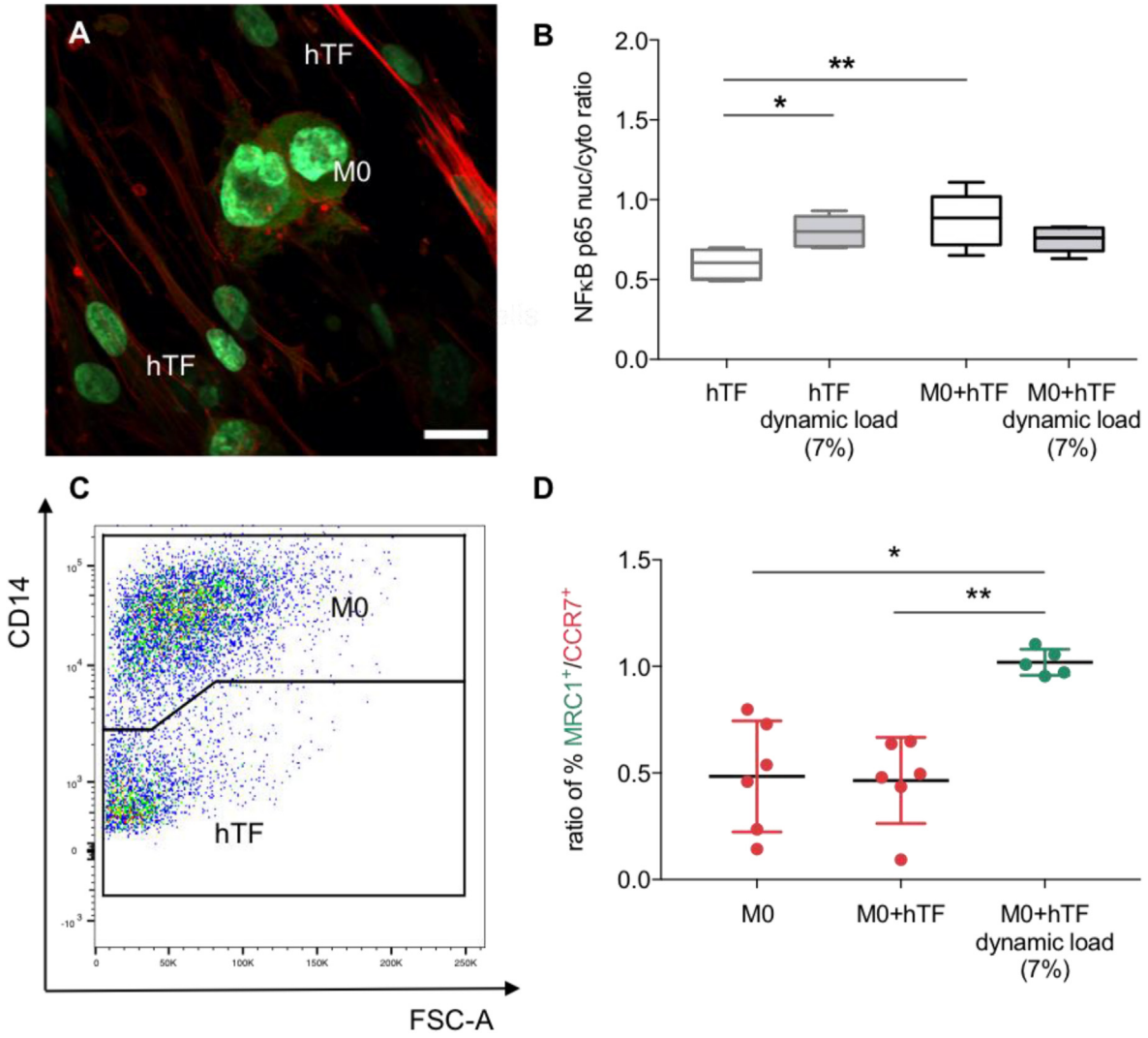


**Fig. 5. Direct co-culture of M0 and hTFs increases nuclear NFκB-p65 translocation in hTFs in vitro.** (A) Immunofluorescent staining of M0 macrophages and hTFs cultured on aligned PCL substrates stained for F-actin (red), DNA (blue) and NFκB-p65 (green). (B) Quantification of nuclear translocation of NFκB-p65 in hTFs revealed significantly increased levels when co-cultured with M0 macrophages. Nevertheless, the nuclear p65 amount was lower in the mechanically stimulated condition (n = 5). (C) Detection of cell populations by flow cytometry was done using CD14 and CD90 staining. CD14 positive and CD90 negative cells indicate macrophages whereas CD90 positive and CD14 negative cells indicate tendon fibroblasts. (D) Further gating of $CD14^+/CD90^-$ cells for their polarization markers $CCR7^+$ (M1-type marker) and $MRC1^+$ (M2-type marker) indicate a trend for a polarization towards anti-inflammatory macrophages if exposed to 7% dynamic loading in direct co-culture. The ratio between $MRC1^+/CCR7^+$ cells revealed a significant increased proportion of $MRC1^+$ positive cells in the dynamically loaded co-culture condition (n = 6). Specifically the percentages of $CCR7^+$ cells were 4.5% for the M0 monoculture, 4.32% for the M0 + hTF co-.culture and 4.745% for the dynamically loaded co-culture. Regarding $MRC1^+$ cells we measured 2.45% for the monoculture, 2.14% for the co-culture and 4.7% for the dynamically loaded co-culture. Statistical analysis was performed using Kruskal Wallis non-parametric ANOVA with Dunn's post-test comparing every treatment and with its corresponding control (hTF, unloaded or M0 on PCL aligned, unloaded respectively) (*P ≤ 0.05, **P ≤ 0.01). Scale bar represents 20 μm. (For interpretation of the references to colour in this figure legend, the reader is referred to the Web version of this article.)

the gene expression level, which were translated into a slight increase in IL1B secretion. Overall, our results on macrophage activation by biomaterial surface topography alone is in agreement with the literature, and underlines this aspect as a potentially important biomaterial design element in patches used for tendon tissue repair [31,40,48,51,54,55]. Also consistent with previous reports [44], we observed increased M1-like activation with dynamic stretching (7% at 1 Hz) in macrophages cultured on randomly oriented topographies. This polarization and expression of inflammatory markers was similar, albeit lower in M0 loaded at dynamic 3% strain (Supplementary Fig. S2). Interestingly, this initial pro-inflammatory activation reverted after longer periods of time in co-culture (48 h, 72 h, Supplementary Fig. S3). Although the precise mechanism has not yet been described, initial experiments using the rho-associated kinase inhibitor Y27632 suggest cell contractility to be important for load-induced polarization (Supplementary Fig. S4).

Our experiments went beyond these previous observations to investigate whether pro-inflammatory effects of mechanical stretch could be overridden by biomaterial surface topology. We found that the observed behavior of macrophages on aligned substrates in static culture (Fig. 1) was significantly changed by dynamic mechanical stimulation of macrophages cultured alone (Fig. 2). Moving further toward potential effects on tissue resident fibroblasts, we analyzed secreted cytokines from mechanically loaded macrophages. We hypothesized that factors secreted by mechanically stimulated macrophages would in turn activate human tendon fibroblasts, and in fact NFκB pathway activation was seen in hTFs exposed to conditioned medium from mechanically loaded macrophage cultures (Fig. 3). When comparing the macrophage

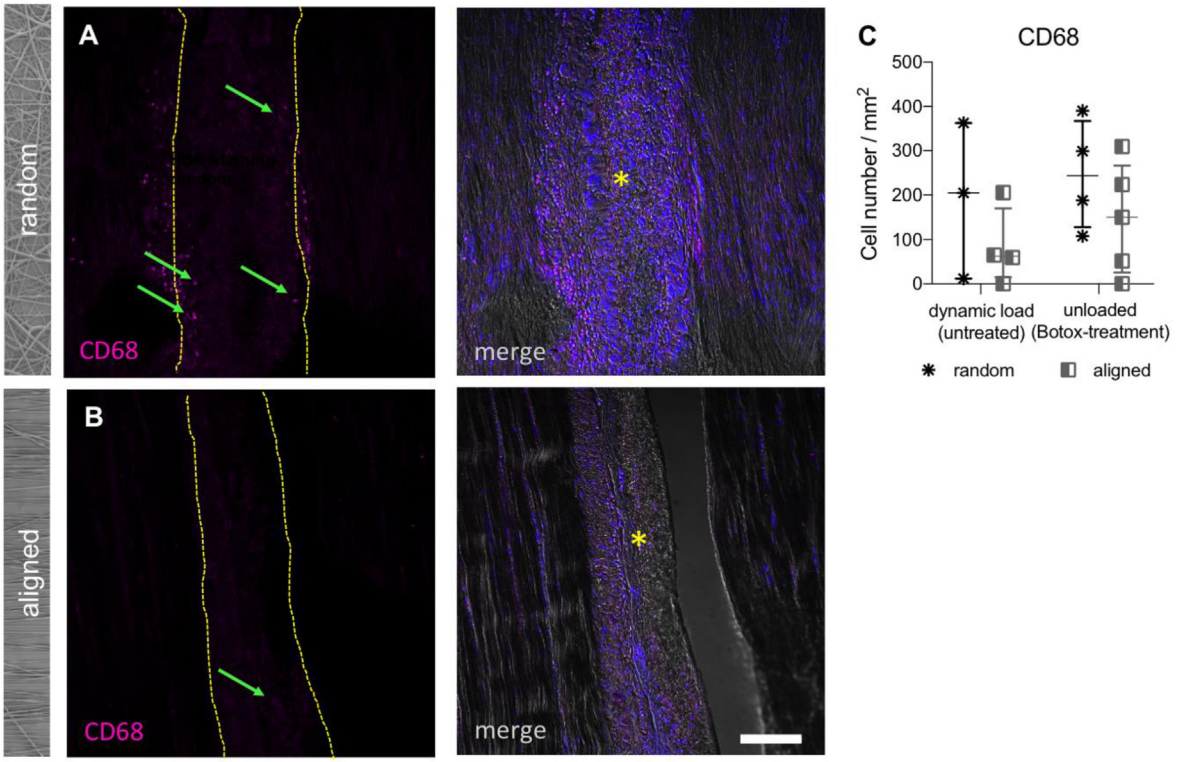


**Fig. 6. Tissue integration of PCL scaffolds with different fiber organizations in vivo.** (A, B) Anti-CD68 staining of randomly oriented (upper panel) and aligned (bottom panel) scaffolds 7 days after their implantation in rat Achilles tendons. Nuclear staining (DAPI, merge, right panel) reveals a large population of host cells in both constructs, with anti-CD68 staining (pink, left panels) qualitatively indicating a higher number of/larger area covered by immune cells in the randomly oriented samples. Yellow dotted lines (asterisk) in A and B marks the position of the scaffolds in the tissue. Scale bar represents 100 μm. (C) Semi-quantitative analysis of cell number per area indicated high variability in the number of stained immune cells around and in the randomly oriented fiber scaffolds, with non-significant but large effects consistent with *in vitro* observations that mechanical unloading and fiber disorganization promote a pro-inflammatory signature. Statistical analysis was performed using Kruskal Wallis non-parametric ANOVA with Dunn's multiple comparisons test to assess the statistical difference between the groups ($p = 0.333$). (For interpretation of the references to colour in this figure legend, the reader is referred to the Web version of this article.)

conditioned medium from both experimental conditions, the assayed cytokine levels were quite variable and no statistical differences were detected. Still, the observed increase in NFκB-p65 translocation suggested that the non-statistically significant increase in TNF and IL1B secretion among other possibly synergistic cytokines [56] was sufficient to provoke the observed pro-inflammatory response, as well as decreased matrix turnover potential (Fig. 3). Furthermore, the intrinsic expression of pro-inflammatory cytokines by the tendon fibroblasts themselves was downregulated, indicating an adaptive mechanism in response to the inflammatory stimulus from the macrophages.

Next, we investigated whether mechanical conditioning of tendon fibroblasts could regulate their activation by exogenously introduced proinflammatory cytokines. We have shown in our previous studies that highly aligned biomaterial surface topographies can mute the inflammatory response of tendon fibroblasts to IL1B [26]. Here, we show that hTFs mechanically challenged for 24 h do not significantly change their gene expression of key matrix turnover genes or tenogenic markers (Supplementary Fig. S5). Although this partially contradicts previously published work, the shorter time points used in our experiments may account for some of this discrepancy [57].

Hypothesizing that mechanical stretch may confer a similar "mechano-protective" effect, we mechanically conditioned hTFs before subsequent stimulation by IL1B. In response to load we observed nuclear elongation in the cells cultured on both constructs (Fig. 4B). Indeed, mechanical loading muted inflammatory activation as indicated by the substantially diminished translocation of the NFκB-p65 subunit to the nucleus (Fig. 4C). In fact, it has been shown that mechanical factors including cell shape and the cellular environment influences the NFκB-p65 localization and oscillation [58,59]. Because this effect has also been reported to be regulated by substrate stiffness [58], we speculate it is related to cytoskeleton-dependent gene regulation [60], as it has been shown to be the case for other factors [61].

To determine if direct contact between tendon fibroblasts and macrophages could be a critical factor in the outcome of the above experiments we performed direct contact co-culture studies on the aligned substrates, focusing on the polarization profile of M0 macrophages as the likely dominant biological outcome [62]. Consistent with the literature using fibroblasts from other tissues, we observed that direct contact co-culture generally led to a decreased fraction of pro-inflammatory macrophages (diminished $CCR7^+$ expression) in direct contact co-culture with tendon fibroblasts. We also made the more novel observation that dynamic mechanical loads further reduced the pro-inflammatory macrophage population, accompanied by increased proportions of M2-like ($MRC1^+$) cell subpopulations within the system. Collectively these observations illuminate non-trivial aspects of macrophage-fibroblast interaction and the regulation of these interactions by direct contact and biophysical cues from their matrix (or biomaterial substrate). Similar anti-inflammatory effects have been described for mesenchymal stromal cells (MSC) of different origins and autologous MSC administration has even been proposed as a therapeutic treatment [63]. Although our study did not reveal the factor or factor combination behind the observed anti-inflammatory response, the increased IL6 production in tenocytes stimulated by macrophage-conditioned media described by others [62] might be, at least partially, responsible [64]. Our results also hint at the potentially central importance of mechanical forces in driving macrophage polarization in a manner consistent with resolution of tissue healing [65–68].

Across this work, our findings were consistent with previous

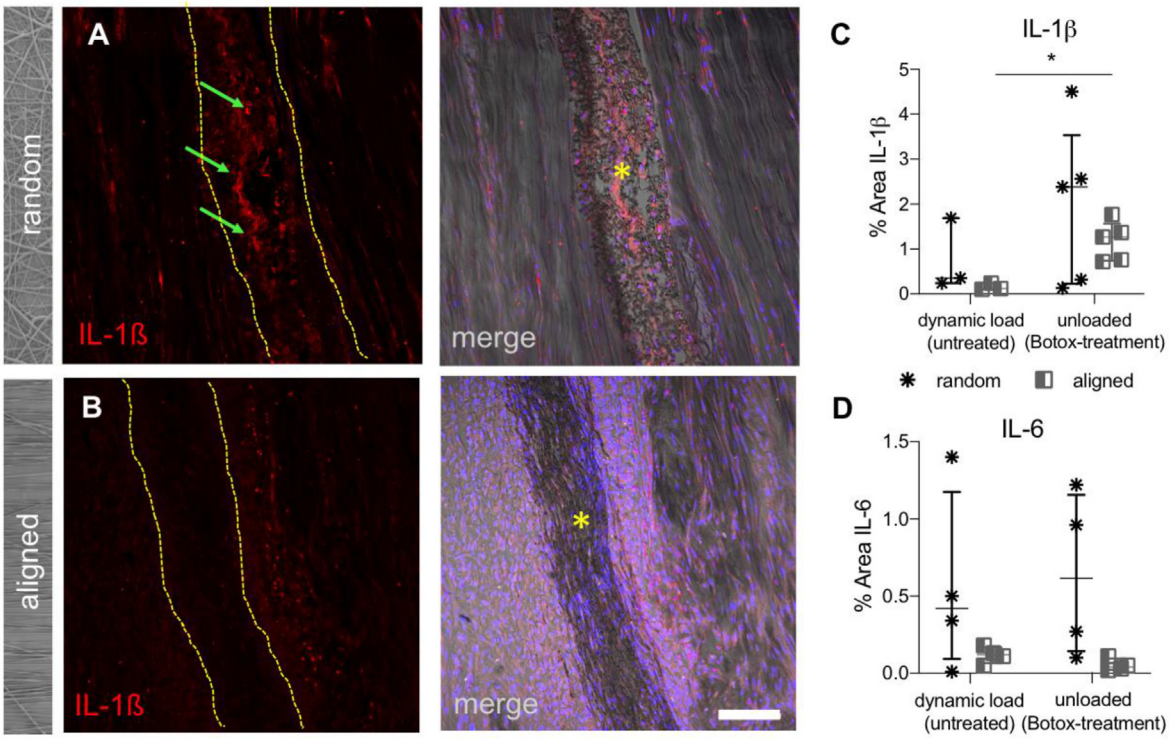


**Fig. 7. Pro-inflammatory cytokine secretion is sensitive to electrospun fiber alignment and muscle forces in vivo.** Representative images of randomly oriented (A) and aligned (B) scaffold (between dashed lines, asterisk) placed in tendons of untreated animals and stained with IL-1β antibody (IL-1β - red signal in left panels, merge of IL-1β signal, DIC and nuclear stain - right panel). (C) Semi-quantitative analysis of IL-1β expression on tissue sections. Significant large effect with increased IL-1β secretion was found by host cells populating aligned scaffolds. Statistical analysis was performed using Mann Whitney test comparing dynamic load (untreated) with the unloaded (Botox treated) group for aligned and random scaffolds, separately. (*$P \leq 0.05$). Scale bars represent 100 μm. (For interpretation of the references to colour in this figure legend, the reader is referred to the Web version of this article.)

literature on mechanical and surface structure regulation of macrophages and tendon cells, individually [19,21,22,40]. Our work represents a knowledge advance in identifying how these individual responses augment and in some cases differ when these biophysical cues are applied in co-culture systems. Among the most striking observations is the manner in which mechanical stimulation initiates a low-level activation of the NFκB pathway in isolated tendon cells, but this same stimulus protects these cells from inflammatory "hyper-activation". Also striking was the degree to which biophysically-driven macrophage polarization was context dependent, particularly with regard to direct contact co-culture that when combined with mechanical loading induced a marked increase in the M2-like macrophage marker MRC1.

We do note that this marker was generally expressed in only a small subset of macrophages (< 5%), and that more thorough analysis of M2 markers would be valuable. In fact, the heavy reliance on only two FACS compatible surface markers to infer the biological relevance of the macrophages is a major limitation that we tried to address by also more comprehensively assaying cytokine expression, and NFκB activation.

We focused on the NFκB pathway as a proxy for "pro-inflammatory activation" since an increase in NFκB signaling has been related to impaired tendon healing [69]. Further, it has been associated with increased pro-inflammatory cytokine expression and innate immune cells within the joint [69]. Therefore, the dynamic activation provides valuable knowledge regarding the outcome after surgical repair together with the analyzed aspects involved in ECM turnover. We focused on IL1B since it has been shown to trigger NFκB pathway activation, however the cytokines involved in the complex processes following injury are likely to be many [69]. The present *in vitro* model provides little mechanistic insights into the role of mechanically challenged biomaterials in mediating cell response. It does however represent an important first step in introducing controlled *in vitro* experimental models (and emergent phenotypes that are clinically/biologically relevant) that can be used to decouple stromal-immune cell cross-talk, laying an essential groundwork for mechanistic study. A further limitation of the study is the use of a cell line (THP-1) as macrophage source. Nevertheless, repeating key experiments with primary monocytes revealed similar behavior compared to the cell line (Supplementary Figs. S6 and S7).

Importantly, the biological relevance of the above *in vitro* investigations was robustly supported by a series of *in vivo* experiments. Here, scaffolds with aligned and random fiber organizations were implanted within the core tendon tissue of the rat Achilles tendon, with the calf muscles of certain experimental groups being paralyzed by injection with Botulinum toxin (Supplementary Fig. S8). These experiments emulated the 'unloaded' situation of the *in vitro* experiments. Cryosectioning and fluorescent staining showed a high density of host cells in the scaffolds 7 days after surgery (Fig. 6). A heightened presence of $CD68^+$ cells in randomly ordered scaffolds was consistent with the pro-inflammatory signature of these materials seen *in vitro* (Fig. 1). Also consistent was that mechanical unloading by Botox treatment led to an increased secretion of pro-inflammatory factors such as IL-1β accompanied by increased expression of matrix degrading enzymes (Fig. 7, Supplementary Fig. S9). These data help to illuminate the link between inflammatory mechanisms and tendon tissue homeostasis.

Taken together, our data consistently support the premise that disorganized PCL topographies provoke an increased inflammatory response, and that macrophage sensitivity to substrate topography and mechanical stimulus can powerfully affect biological outcomes that are relevant to tissue repair. The fact that mechano-sensitive response of macrophages in our models generally outweighed that of tendon fibroblasts was striking, and highlights a plausible role for macrophages

as centrally important mechano-sensors that regulate tendon repair. This potential role of macrophages appears to be underappreciated in the literature regarding tendon repair. Our findings thus identify and describe an important vector by which mechanical cues mediate healing outcome after biomaterial implantation.

## 4. Conclusion

Using a novel *in vitro* model of tendon stromal-immune co-culture, with strong support from accompanying *in vivo* rat model experiments, we demonstrate the impact of topographical and mechanical cues on early host-biomaterial interactions. We observed a profound response of naïve macrophages to these stimuli, with strong effects on tendon cells in indirect and direct co-culture. Strikingly, quantification of macrophage response to mechanical loading was found to promote a pronounced phenotypic switch towards an M2-like phenotype, a switch that is widely considered to be beneficial for tissue healing. These findings suggest that macrophages may play an important role as mechano-sensitive cells that modulate tendon healing. These insights gained from a mechanically challenged model of stromal and immune cell cross-talk inform our understanding of tissue repair, and highlight how readily-controlled biomaterial design factors can integrate and steer complex biological processes to divergent tissue repair outcomes.

## 5. Materials and methods

### 5.1. Electrospun polycaprolactone nanofiber substrates

Electrospun polycaprolactone (PCL) nanofiber membranes with aligned and random orientation (Nanofiber solutions; NanoECM™, NanoAligned™) were cut into strips (28 × 8 mm), soaked in 80% ethanol for 1 h, washed with PBS and dried overnight in the incubator (37 °C, 5% $CO_2$). Following, the substrates were coated with collagen 1 solution (50 μg/ml, according to the previous described recipe [70]) and incubated for 18 h at 37 °C. Prior to cell seeding, the substrates were washed with PBS and incubated with RPMI medium for 4 h.

### 5.2. Tissue collection and isolation of human tendon fibroblasts

Healthy hamstring tendons were obtained from male patients undergoing surgical reconstruction of the anterior cruciate ligament. Tissue collection received ethical permission of the Canton of Zurich (permission number 2015-0089). Human tendon fibroblasts (hTFs) were isolated from the tissues following a previously described protocol [71]. First, the tissue samples were cleared from surrounding tissue, trimmed into small pieces before digesting the extracellular matrix (ECM) using collagenase D (Roche) for 6 h at 37 °C. Isolated cells were cultured in DMEM/F12 (Sigma) supplemented with 20% fetal bovine serum (FBS, Sigma), 1% penicillin-streptomycin (P/S, Sigma) and 1% amphotericin B (Gibco). When 80% confluence was reached cells were cryopreserved in liquid nitrogen in 70% DMEM/F12, 20% FBS and 10% DMSO (Sigma). The experiments in this study were performed with thawed and expanded hTFs at passage 2.

### 5.3. Macrophage differentiation

The human monocyte THP-1 cell line was obtained from ATCC (American Type Culture Collection) and cultured in RPMI culture medium (Sigma) supplemented with 10% FBS and 1% P/S at 37 °C in a humified 5% $CO_2$ atmosphere. Subculturing was performed routinely before the cell density reached 1 × $10^6$ cells/ml. Differentiation of monocytes towards naïve macrophages (M0) was induced by stimulating with 100 nM phorbol 12-myristate 13-acetate (PMA, Sigma) for 3 days, followed by 24 h cultivation with PMA-free fresh RPMI medium [72,73]. The M1 phenotype was chemically provoked by stimulating the naïve macrophages with 20 ng Interferon-γ (IFN-γ; Miltenyi Biotec) and 100 ng LPS (Lipopolysaccharide; Sigma), while the M2 phenotype was triggered by 20 ng Interleukin-4 (IL-4; Miltenyi Biotec) stimulation for 24 h. The validation of a successful chemical polarization was performed by measuring specific surface markers CCR7 (M1) and MRC1 (M2) on the gene expression and protein level. For experiments, naïve (M0) macrophages were cultured on collagen coated tissue culture plastic (TCP) or electrospun PCL nanofiber substrates at a density of 100,000 cells/$cm^2$ and submerged in 3 ml of culture medium.

### 5.4. Tendon fibroblast and macrophages culture and mechanical stimulation

Primary hTFs were seeded on aligned and random PCL nanofiber substrates at a density of 25,000 cells/$cm^2$ for 24 h before conditioning with mechanical load. M0 macrophages and hTFs were co-cultured in RPMI medium at a ration of 4:1 (M0:hTF; 100,000 cells/$cm^2$ THP-1: 25,000 cells/$cm^2$ hTFs) since the hTFs further proliferate in culture to finally reach a similar number as the macrophages.

The hTFs were mechanically conditioned after 24 h of culturing on the substrates while the THP-1 were primarily differentiated to M0 macrophages (4 days) before the stimulation. For mechanical stimulation, cells adhering to PCL substrates were clamped within a custom-made bioreactor for conditioning by either static load (1% strain) or dynamic loading (7% strain) for 24 h. The dynamic loading protocol consists of 8 h of 7% dynamic loading at 1 Hz followed by 16 h resting period.

### 5.5. RNA isolation and quantitative real-time PCR

RNA isolation from hTFs and macrophages was performed by adding 500 μl QIAzol Lysis Reagent (Qiagen, Switzerland) to the previously PBS washed cells. Briefly, chloroform was added to the samples to induce the phase separation according to the manufacturer instructions. The quality and quantity of the RNA remaining in the aqueous phase was analyzed using a Take 3 spectrophotometer (BioTek, Switzerland). From 9 ng of total RNA complementary DNA (cDNA) was synthesized in a volume of 20 μl using High Capacity RNA-to-cDNA Kit (Thermo Scientific, Switzerland). Gene expression analysis of matrix turnover genes in hTF and phenotype indicating surface markers in macrophages was performed after mechanical stimulation by real time qPCR. Each qPCR reaction was composed of 2 μl cDNA and 8 μl of Mastermix (5 μl TaqMan® Universal PCR Master Mix, 0.5 μl of forward and reverse TaqMan primer, 2.5 μl of ultrapure water) adding up to a total volume of 10 μl. In the StepOne thermocycler (Applied Biosystems) the samples were amplified after initial 10 min at 95 °C in 40 cycles of 95 °C for 15 s and 60 °C for 1 min. Technical duplicates were measured for each sample and for the quantification the comparative $2^{-\Delta CT}$ method was chosen with glyceraldehyde 3-phosphate dehydrogenase (*GAPDH*) as a reference gene. The relative gene expression levels were normalized to hTFs or M0 macrophages cultured on unloaded, random or aligned substrates in RPMI medium.

### 5.6. Flow cytometry measurement

Macrophages were harvested using Accutase (Sigma) and transferred to a 1.5 ml tube (Eppendorf). Briefly, cells were washed once and resuspended in 100 μl PBS containing the antibody mix. The conjugated antibodies M1 polarization marker CD197 (CCR7) Alexa Fluor 647 (BD Bioscience) and M2 polarization marker CD206 (MRC1) FITC (BD Bioscience) were incubated for 20 min at 4 °C in the dark. Antibody mixes also contained Live/Dead® violet (0.25 μg/ml cell suspension) in order to exclude dead cells from the analysis. After incubation, samples were washed with FACS buffer (1% BSA in PBS) and resuspended in 500 μl PBS before transferring into FACS tubes (Falcon). Samples were kept on ice at 4 °C in the dark until measurement. Data collection was performed using Fortessa device with FACS Diva software (Becton

Dickinson, San Jose, CA, USA) and analyzed using FlowJo software (TreeStar Inc., Ashland, OR, USA).

### 5.7. Scanning electron microscopy

Samples were fixed in 4% formaldehyde (Sigma) for 30 min at room temperature and dehydrated by an ascending series of ethanol (from 50 to 100%), following a 5 min treatment with to hexamethyldisiloxane (HMDSO, 205,389, Sigma). After air-drying overnight samples were sputter coated with a 5 nm gold-palladium layer (high vacuum coater Leica EM ACE 600, Switzerland). The Hitachi S-4800 scanning electron microscope (Hitachi High-Technologies Corporation, Japan) was used to acquire images of the cells cultured on the different substrates at an acceleration voltage of 5 kV and 10 μA current, with a magnification up to 15,000 times.

### 5.8. Immunofluorescent staining, image acquisition and analysis

Mechanically and chemically stimulated nuclear translocation of NFκB p65 in hTFs was assessed by staining for the p65 subunit of NFκB. Briefly, samples were washed with PBS and fixed in 4% formaldehyde (Sigma) for 20 min at room temperature. Next, cells were permeabilized with 0.2% Triton-X in PBS for 5 min before incubation for 1 h with the primary anti-p65 mouse monoclonal antibody (1:50, sc-8008, Santa Cruz Biotechnology, Germany). After three washing steps, cells were incubation with Alexa Fluor 488-conjugated anti-mouse IgG (1:200, A21202, Thermo Fisher) secondary antibody together with SiR-actin (1:250, SC001, SpiroChrome). After the 1 h incubation, cell washed three times and mounted using Immu-Mount™ (Thermo Scientific Shandon, Cat# 10662815, United States). The same staining procedure was applied in hTFs cultured on aligned PCL substrates after they were stimulated for 30 min with conditioned medium from macrophages exposed to different mechanical loading protocols and furthermore after additional 15 min of chemical stimulation by 5 ng/ml IL1B. Cell nuclear morphology was quantified for hTFs stained with NucBlue™ (Nucleus) calculating the aspect ratio (major axis/minor axis) using a Fiji and associated plugins [74].

The polarization profile of M0 macrophages on PCL nanofiber substrates was assessed using the staining protocol as described above with the primary antibodies CCR7 (1:200, ab32527, rabbit, Thermo Fischer, Switzerland) for the M1 surface marker and MRC1 (1:50, MCA2155, mouse, Thermo Fischer, Switzerland) for the M2 surface marker. Next, cells were incubated with the secondary antibodies Alexa488 (1:1000, A-21206, donkey anti-Rabbit, Thermo Fischer, Switzerland) for the M1 surface marker, Alexa Fluor 647 (1:1000, A-21235, goat anti-Mouse, Thermo Fischer, Switzerland) for the M2 respectively and NucBlue™ reagent (1 drop/ml, R37606, Thermo Fischer, Switzerland) for the cell nuclei.

Imaging was performed using a spinning disc confocal microscope equipped with a 10x and a 60x 1.35 N A. oil-immersion objective. Co-culture images were acquired using a Nikon (Nikon eclipse Ti2-A, Nikon Instruments Europe B.V.) equipped with a 60x objective. ImageJ software (version 2.0.0-rc-15) was used to quantify the NFκB p65 signal within the nucleus (p65 nuc) and in the cytoplasm (p65 cyto). More precisely, the ratio of p65 within the nucleus compared to the cytoplasm was calculated by measuring the fluorescence intensity in both compartments for 8 cells per condition and time point.

The explanted tissue of the *in vivo* experiments was fixed in 4% paraformaldehyde in PBS for 24 h and subsequently washed in PBS 3x for 1 h and cryo-preserved in 30% sucrose in PBS embedded in cryomedium (Surgipath Cryogel®, Leica Microsystems, Vienna, Austria). Subsequently, 12 μm cryosections were prepared using a Leica CM1950 cryostat.

For immunohistochemmical staining, the sections were washed in PBS for 5 min and blocked with 1% bovine serum albumin in PBS for 15 min. The antibodies were diluted in the same buffer (CD68: Novus Bio NB100-683, 1:30; IL1-β: Proteintech 66,737-1-lg, 1:100; IL6 Abcam ab6672, 1:100; MMP1: Proteintech10371-2-AP, 1:100; MMP2: Proteintech 66366-1-Ig, 1:100; MMP3: Proteintech 66338-1-Ig, 1:200; MMP13: Proteintech 18165-1-AP, 1:100) and incubated in a wet chamber at 4 °C for 12 h. After 3 washing steps in PBS (5 min), the sections were incubated with corresponding secondary antibodies (Alexa488-, Alexa568-, or Alexa647 1:500; Invitrogen, Karlsruhe, Germany) and 4,6-Diamidino-2phenylindol dihydrochlorid (DAPI, 1:500) for 1 h at room temperature. After 3 washing steps in PBS, the sections were embedded in FluoromountTM Aqueous Mounting Medium (Sigma Aldrich, Vienna, Austria) and preceded to microscopic analysis. Confocal imaging was performed using a LSM 700 confocal microscope (Zeiss), image acquisition was done with ZEN 2010 (Zeiss), and image dimensions were 1024 × 1024 pixels with an image depth of 16 bit. Two times averaging was applied during image acquisition. Laser power and gain were adjusted to avoid saturation of single pixels. All images were taken using identical microscope settings based on the secondary antibody control stainings. Antibody signals were semi-quantitatively analyzed by ImageJ software. For CD68, number of positive cells/mm2 was analyzed, for all other (secreted) proteins, % area was analyzed as previously published (PMID: 29672303).

### 5.9. ELISA assay

Conditioned medium from macrophages exposed to different substrate topographies and mechanical loading protocols was collected after 24 h of loading. Quantification of IL-6, TNF, IL1β, IFN-γ, IL-13, IL-4, IL-8, MCP-1, MDC and SDF-1a was performed using a custom made Meso Scale Discovery U-PLEX human biomarkers (Meso Scale Discovery) according to the manufacturer's instructions. Plates were read using the MESO™ QuickPlex SQ 120 imager (Meso Scale Discovery).

### 5.10. Animal experiments

All animal experiments and procedures were conducted in accordance with Austrian laws and were approved by regulatory authorities on animal experimentation (permit number BMWFW-66.019/0038-V/3b/2019).

A total of 18 male Sprague Dawley rats (age 12 weeks, Janvier Labs, Le Genest-Saint-Isle, France) were included in the study. For scaffold implantation, the Achilles tendon was exposed by a dorsal skin incision and a standardized 5 mm incision was created in the Achilles tendon. Subsequently, the scaffold was implanted press-fit without any additional fixation. The skin was then closed using sutures.

In 6 animals, the oriented scaffold was implanted into the right Achilles tendon and the non-oriented scaffold was inserted into the left Achilles tendon. An additional 12 animals were treated with Clostridium botulinum Toxin Typ A (Botox, Allergan, Frankfurt, Germany). Therefore, under general anesthesia 1IU in 50 μl sterile saline was injected into each the M. gastrocnemius lateralis and medialis, as well as into the M. soleus muscle. 4 days after the injection scaffold implantation was performed as described. 7d post-surgery the animals were euthanized by intracardial barbiturate injection under general anesthesia and the Achilles tendons were harvested, fixed in 4% paraformaldehyde in PBS for 24 h at 4 °C, and subsequently processed for cryosectioning.

### 5.11. Statistical analysis

The Kruskal Wallis non-parametric ANOVA with Dunn's post-test was performed to analyze the impact of topography cues on M0 macrophages by comparing them after cultivating on random oriented and aligned PCL substrates compared with its control (M0 on TCP) *in vitro* using GraphPad Prism (version 7.0a). Gene expression results are presented as relative expression of hTFs and macrophages cultured on the

different substrates and exposed to the mechanical stimulation normalized to corresponding control by dividing through the median of the control (hTFs cultured on TCP or unloaded PCL). Statistical analysis of the gene expression data as well as the differences between nuclear-to-cytoplasmic p65 ratios was performed using two-way ANOVA with Tukey's post hoc test and Kruskal Wallis non-parametric ANOVA with Dunn's post hoc multiple comparison method, comparing every treatment and with its corresponding control using GraphPad Prism (version 7.0a). In addition, a Kruskal Wallis non-parametric ANOVA with Dunn's post-test was performed to compare the nuclear translocation of p65 in dynamically loaded hTFs to the unloaded control. The data on the protein level acquired by flow cytometry or UPLEX ELISA was analyzed by Kruskal Wallis non-parametric ANOVA with Dunn's post hoc multiple comparison method to investigate the effect of topographical cues (random, aligned PCL scaffolds) or mechanical loading (1%, 7% strain) in regard to TCP or unloaded samples, respectively. The results are displayed as median ± range of several independent experiments (n represents a new thawed macrophage aliquot and/or tendon donor) and are considered statistically significantly different when $*p \leq 0.05$.

## Notes

The authors declare no conflict of interest.

## FUNDING

This research did not receive any specific grant from funding agencies in the public, commercial, or not-for-profit sectors.

## Data availability

The raw/processed data required to reproduce these findings cannot be shared at this time due to technical or time limitations.

## Acknowledgments

Thanks to Stefania Wunderli for sharing her knowledge and help in using the bioreactor. A special thanks goes to Chiara Griffoni at Empa St. Gallen for helping me to isolate the primary monocytes from the blood. Thanks to Stefanie Guimond at Empa St. Gallen for her help to acquire the SEM images. A special thanks also goes to Elias Bachmann for providing essential contribution by helping with the mechanical testing of the scaffolds. Further, we would like to thank Stefan Dudli for generously providing the THP1-XBlue™-CD14 cells. We would further like to acknowledge the contribution of the Swiss Center for Musculoskeletal Biobanking (SCMB) by allowing us to use their Nikon confocal microscope. Thanks also to the Flow cytometry facility from the University of Zurich for their support in the FACS experiments.

## Appendix A. Supplementary data

Supplementary data to this article can be found online at https://doi.org/10.1016/j.biomaterials.2020.120034.

## ABBREVIATIONS

| | |
|---|---|
| CCR7 | C-C chemokine receptor type 7 |
| CD14 | Cluster of differentiation 14 |
| CD248 | Cluster of differentiation 248 |
| CD90 | Cluster of differentiation 90 |
| CD68 | Cluster of differentiation 68 |
| CM | Macrophage conditioned medium |
| COL1 | Collagen type 1 |
| COL3 | Collagen type 3 |
| DNA | Deoxyribonucleic acid |
| FSC-A | Forward scatter area |
| hTF | Human tendon fibroblast |
| IFN-γ | Interferon-gamma |
| IL1B | Interleukin-1beta |
| IL-6 | Interleukin-6 |
| MKX | Mohawk |
| MMP1 | Matrix metalloproteinase 1 |
| MMP3 | Matrix metalloproteinase 3 |
| MMP13 | Matrix metalloproteinase 13 |
| MSC | mesenchymal stem cell |
| MRC1 | Mannose receptor C-type 1 |
| NFκB-p65 | Nuclear factor 'kappa-light-chain-enhancer' of activated B-cells subunit p65 |
| PCL | Polycaprolactone |
| PDPN | Podoplanin |
| ROCK | Rho kinase |
| SCX | Scleraxis |
| TCP | Tissue culture plastic |
| TGFB1 | Transforming growth factor beta-1 |
| TNF | Tumor necrosis factor alpha |
| VCAM1 | Vascular cell adhesion protein 1 |

## References

[1] M.H. Amini, E.T. Ricchetti, J.P. Iannotti, K.A. Derwin, An update on scaffold devices for rotator cuff repair, Tech. Shoulder Elbow Surg. (2017), https://doi.org/10.1097/BTE.0000000000000122.
[2] O. Hakimi, P.A. Mouthuy, A. Carr, Synthetic and degradable patches: an emerging solution for rotator cuff repair, Int. J. Exp. Pathol. 94 (2013) 287–292, https://doi.org/10.1111/iep.12030.
[3] D. Kovacevic, S.A. Rodeo, Biological augmentation of rotator cuff tendon repair, Clin. Orthop. Relat. Res. (2008), https://doi.org/10.1007/s11999-007-0112-4.
[4] G. Deprés-tremblay, A. Chevrier, M. Snow, M.B. Hurtig, S. Rodeo, M.D. Buschmann, Rotator cuff repair: a review of surgical techniques, animal models, and new technologies under development, J. Shoulder Elbow Surg. (2016), https://doi.org/10.1016/j.jse.2016.06.009.
[5] K. a Derwin, A.R. Baker, R.K. Spragg, D.R. Leigh, J.P. Iannotti, Commercial extracellular matrix scaffolds for rotator cuff tendon repair, J Bone Jt. Surg Am. 88 (2006) 2665–2672, https://doi.org/10.2106/JBJS.E.01307.
[6] E.T. Stace, S. Tiberwel, A.J. Carr, N.S. Nagra, W. Khan, The use of electrospun scaffolds in musculoskeletal tissue engineering: a focus on tendon and the rotator cuff, Curr. Stem Cell Res. Ther. (2018), https://doi.org/10.2174/1574888x13666180129105707.
[7] E.M. Christenson, K.S. Anseth, J.J.J.P. Van den Beucken, C.K. Chan, B. Ercan, J.A. Jansen, C.T. Laurencin, W.J. Li, R. Murugan, L.S. Nair, S. Ramakrishna, R.S. Tuan, T.J. Webster, A.G. Mikos, Nanobiomaterial applications in orthopedics, J. Orthop. Res. (2007), https://doi.org/10.1002/jor.20305.
[8] W.J. Li, R.L. Mauck, J.A. Cooper, X. Yuan, R.S. Tuan, Engineering controllable anisotropy in electrospun biodegradable nanofibrous scaffolds for musculoskeletal tissue engineering, J. Biomech. (2007), https://doi.org/10.1016/j.jbiomech.2006.09.004.
[9] Z. Ma, M. Kotaki, R. Inai, S. Ramakrishna, Potential of nanofiber matrix as tissue-engineering scaffolds, Tissue Eng. (2005), https://doi.org/10.1089/ten.2005.11.101.
[10] S.B. Orr, A. Chainani, K.J. Hippensteel, A. Kishan, C. Gilchrist, N.W. Garrigues, D.S. Ruch, F. Guilak, D. Little, Aligned multilayered electrospun scaffolds for rotator cuff tendon tissue engineering, Acta Biomater. (2015), https://doi.org/10.1016/j.actbio.2015.06.010.
[11] Y.Z. Zhang, J. Venugopal, Z.M. Huang, C.T. Lim, S. Ramakrishna, Characterization of the surface biocompatibility of the electrospun PCL-Collagen nanofibers using fibroblasts, Biomacromolecules (2005), https://doi.org/10.1021/bm050314k.
[12] G.H. Kim, Electrospun PCL nanofibers with anisotropic mechanical properties as a biomedical scaffold, Biomed. Mater. 3 (2008) 25010, https://doi.org/10.1088/1748-6041/3/2/025010.
[13] M.A. Woodruff, D.W. Hutmacher, The return of a forgotten polymer - polycaprolactone in the 21st century, Prog. Polym. Sci. (2010), https://doi.org/10.1016/j.progpolymsci.2010.04.002.
[14] R.R. Duling, Mechanical characterization of electrospun polycaprolactone (PCL): a potential scaffold for tissue engineering, J. Biomech. Eng. 130 (2008) 011006, , https://doi.org/10.1115/1.2838033.
[15] A.J. Engler, S. Sen, H.L. Sweeney, D.E. Discher, Matrix elasticity directs stem cell lineage specification, Cell 126 (2006) 677–689, https://doi.org/10.1016/j.cell.2006.06.044.
[16] R.I. Sharma, J.G. Snedeker, Biochemical and biomechanical gradients for directed bone marrow stromal cell differentiation toward tendon and bone, Biomaterials 31 (2010) 7695–7704, https://doi.org/10.1016/j.biomaterials.2010.06.046.
[17] T. Razafiarison, C.N. Holenstein, T. Stauber, M. Jovic, E. Vertudes, M. Loparic, M. Kawecki, L. Bernard, U. Silvan, J.G. Snedeker, Biomaterial surface energy-driven ligand assembly strongly regulates stem cell mechanosensitivity and fate on very soft substrates, Proc. Natl. Acad. Sci. Unit. States Am. 115 (2018) 4631, https://doi.

org/10.1073/pnas.1704543115 LP – 4636.
[18] Z. Yin, X. Chen, J.L. Chen, W.L. Shen, T.M. Hieu Nguyen, L. Gao, H.W. Ouyang, The regulation of tendon stem cell differentiation by the alignment of nanofibers, Biomaterials (2010), https://doi.org/10.1016/j.biomaterials.2009.11.083.
[19] Z. Yin, X. Chen, H. xin Song, J. jie Hu, Q. mei Tang, T. Zhu, W. liang Shen, J. lin Chen, H. Liu, B.C. Heng, H.W. Ouyang, Electrospun scaffolds for multiple tissues regeneration invivo through topography dependent induction of lineage specific differentiation, Biomaterials 44 (2015) 173–185, https://doi.org/10.1016/j.biomaterials.2014.12.027.
[20] W. Wang, J. He, B. Feng, Z. Zhang, W. Zhang, G. Zhou, Y. Cao, W. Fu, W. Liu, Aligned nanofibers direct human dermal fibroblasts to tenogenic phenotype in vitro and enhance tendon regeneration in vivo, Nanomedicine (2016), https://doi.org/10.2217/nnm.16.24.
[21] T. Popielarczyk, A. Nain, J. Barrett, Aligned nanofiber topography directs the tenogenic differentiation of mesenchymal stem cells, Appl. Sci. 7 (2017) 59, https://doi.org/10.3390/app7010059.
[22] K. Zhou, B. Feng, W. Wang, Y. Jiang, W. Zhang, G. Zhou, T. Jiang, Y. Cao, W. Liu, Nanoscaled and microscaled parallel topography promotes tenogenic differentiation of asc and neotendon formation in vitro, Int. J. Nanomed. 13 (2018) 3867–3881, https://doi.org/10.2147/IJN.S161423.
[23] K.K. Zhang, C. Liu, Y.L. Sun, Aligned collagen scaffolds enhance tenogenic differentiation of bone marrow-derived stem cells, Key Eng. Mater. 773 (2018) 333–337 https://doi.org/10.4028/www.scientific.net/kem.773.333.
[24] J. Huang, Y. Chen, C. Tang, Y. Fei, H. Wu, D. Ruan, M.E. Paul, X. Chen, Z. Yin, B.C. Heng, W. Chen, W. Shen, The relationship between substrate topography and stem cell differentiation in the musculoskeletal system, Cell. Mol. Life Sci. 76 (2019) 505–521, https://doi.org/10.1007/s00018-018-2945-2.
[25] N.M. Lee, C. Erisken, T. Iskratsch, M. Sheetz, W.N. Levine, H.H. Lu, Polymer fiber-based models of connective tissue repair and healing, Biomaterials 112 (2017) 303–312, https://doi.org/10.1016/j.biomaterials.2016.10.013.
[26] A.D. Schoenenberger, J. Foolen, P. Moor, U. Silvan, J.G. Snedeker, Substrate fiber alignment mediates tendon cell response to inflammatory signaling, Acta Biomater. 71 (2018) 306–317, https://doi.org/10.1016/j.actbio.2018.03.004.
[27] C. Rinoldi, M. Costantini, E. Kijeńska-Gawrońska, S. Testa, E. Fornetti, M. Heljak, M. Ćwiklińska, R. Buda, J. Baldi, S. Cannata, J. Guzowski, C. Gargioli, A. Khademhosseini, W. Swieszkowski, Tendon tissue engineering: effects of mechanical and biochemical stimulation on stem cell alignment on cell-laden hydrogel yarns, Adv. Healthc. Mater. (2019) 1–10, https://doi.org/10.1002/adhm.201801218 1801218.
[28] A. Scott, J.L. Cook, D.A. Hart, D.C. Walker, V. Duronio, K.M. Khan, Tenocyte responses to mechanical loading in vivo: a role for local insulin-like growth factor 1 signaling in early tendinosis in rats, Arthritis Rheum. (2007), https://doi.org/10.1002/art.22426.
[29] J. Zhang, J.H.C. Wang, Mechanobiological response of tendon stem cells: implications of tendon homeostasis and pathogenesis of tendinopathy, J. Orthop. Res. 28 (2010) 639–643, https://doi.org/10.1002/jor.21046.
[30] J.G. Snedeker, J. Foolen, Tendon injury and repair – a perspective on the basic mechanisms of tendon disease and future clinical therapy, Acta Biomater. (2017), https://doi.org/10.1016/j.actbio.2017.08.032.
[31] N. Jain, V. Vogel, Spatial confinement downsizes the inflammatory response of macrophages, Nat. Mater. 17 (2018) 1134–1144, https://doi.org/10.1038/s41563-018-0190-6.
[32] R. Klopfleisch, Macrophage reaction against biomaterials in the mouse model – phenotypes, functions and markers, Acta Biomater. 43 (2016) 3–13, https://doi.org/10.1016/j.actbio.2016.07.003.
[33] P.J. Murray, J.E. Allen, S.K. Biswas, E.A. Fisher, D.W. Gilroy, S. Goerdt, S. Gordon, J.A. Hamilton, L.B. Ivashkiv, T. Lawrence, M. Locati, A. Mantovani, F.O. Martinez, J.L. Mege, D.M. Mosser, G. Natoli, J.P. Saeij, J.L. Schultze, K. Shirey, A. Sica, J. Suttles, I. Udalova, J.A. vanGinderachter, S.N. Vogel, T.A. Wynn, Macrophage activation and polarization: nomenclature and experimental guidelines, Immunity 41 (2014) 14–20, https://doi.org/10.1016/j.immuni.2014.06.008.
[34] A.D. Lynn, S.J. Bryant, Phenotypic changes in bone marrow-derived murine macrophages cultured on PEG-based hydrogels activated or not by lipopolysaccharide, Acta Biomater. 7 (2011) 123–132, https://doi.org/10.1016/j.actbio.2010.07.033.
[35] L.M. Chamberlain, D. Holt-Casper, M. Gonzalez-Juarrero, D.W. Grainger, Extended culture of macrophages from different sources and maturation results in a common M2 phenotype, J. Biomed. Mater. Res. 103 (2015) 2864–2874, https://doi.org/10.1002/jbm.a.35415.
[36] L. Chung, D.R. Maestas, F. Housseau, J.H. Elisseeff, Key players in the immune response to biomaterial scaffolds for regenerative medicine, Adv. Drug Deliv. Rev. (2017), https://doi.org/10.1016/j.addr.2017.07.006.
[37] Z. Julier, A.J. Park, P.S. Briquez, M.M. Martino, Promoting tissue regeneration by modulating the immune system, Acta Biomater. (2017), https://doi.org/10.1016/j.actbio.2017.01.056.
[38] F.Y. McWhorter, C.T. Davis, W.F. Liu, Physical and mechanical regulation of macrophage phenotype and function, Cell. Mol. Life Sci. (2015), https://doi.org/10.1007/s00018-014-1796-8.
[39] E.T. Ricchetti, A. Aurora, J.P. Iannotti, K.A. Derwin, Scaffold devices for rotator cuff repair, J. Shoulder Elbow Surg. 21 (2012) 251–265, https://doi.org/10.1016/j.jse.2011.10.003.
[40] R. Sridharan, A.R. Cameron, D.J. Kelly, C.J. Kearney, F.J. O'Brien, Biomaterial based modulation of macrophage polarization: a review and suggested design principles, Mater. Today 18 (2015) 313–325, https://doi.org/10.1016/j.mattod.2015.01.019.
[41] S.L. Wunderli, J. Widmer, N. Amrein, J. Foolen, U. Silvan, O. Leupin, J.G. Snedeker, Minimal mechanical load and tissue culture conditions preserve native cell phenotype and morphology in tendon—a novel ex vivo mouse explant model, J. Orthop. Res. 36 (2018) 1383–1390, https://doi.org/10.1002/jor.23769.
[42] F.Y. McWhorter, T. Wang, P. Nguyen, T. Chung, W.F. Liu, Modulation of macrophage phenotype by cell shape, Proc. Natl. Acad. Sci. Unit. States Am. (2013), https://doi.org/10.1073/pnas.1308887110.
[43] S. Korntner, N. Kunkel, C. Lehner, R. Gehwolf, P. Augat, D. Stephan, V. Heu, H. Bauer, A high-glucose diet affects Achilles tendon healing in rats, Sci. Rep. (2017) 1–12, https://doi.org/10.1038/s41598-017-00700-z.
[44] V. Ballotta, A. Driessen-Mol, C.V.C. Bouten, F.P.T. Baaijens, Strain-dependent modulation of macrophage polarization within scaffolds, Biomaterials 35 (2014) 4919–4928, https://doi.org/10.1016/j.biomaterials.2014.03.002.
[45] J. Pugin, I. Dunn, P. Jolliet, D. Tassaux, J.L. Magnenat, L.P. Nicod, J.C. Chevrolet, Activation of human macrophages by mechanical ventilation in vitro, Am. J. Physiol. 275 (1998) L1040–L1050, https://doi.org/10.1152/ajplung.1998.275.6.L1040.
[46] L.A. Matheson, N.J. Fairbank, G.N. Maksym, J.P. Santerre, R.S. Labow, Characterization of the FlexcellTM UniflexTM cyclic strain culture system with U937 macrophage-like cells, Biomaterials (2006), https://doi.org/10.1016/j.biomaterials.2005.05.070.
[47] Z. Wang, W.J. Lee, B.T.H. Koh, M. Hong, W. Wang, P.N. Lim, J. Feng, L.S. Park, M. Kim, E.S. Thian, Functional regeneration of tendons using scaffolds with physical anisotropy engineered via microarchitectural manipulation, Sci. Adv. 4 (2018) eaat4537, https://doi.org/10.1126/sciadv.aat4537.
[48] A. Vishwakarma, N.S. Bhise, M.B. Evangelista, J. Rouwkema, M.R. Dokmeci, A.M. Ghaemmaghami, N.E. Vrana, A. Khademhosseini, Engineering immunomodulatory biomaterials to tune the inflammatory response, Trends Biotechnol. 34 (2016) 470–482, https://doi.org/10.1016/j.tibtech.2016.03.009.
[49] A. Curtis, C. Wilkinson, Topographical control of cells, Biomaterials (1997), https://doi.org/10.1016/S0142-9612(97)00144-0.
[50] S. Chen, J.A. Jones, Y. Xu, H.Y. Low, J.M. Anderson, K.W. Leong, Characterization of topographical effects on macrophage behavior in a foreign body response model, Biomaterials 31 (2010) 3479–3491, https://doi.org/10.1016/j.biomaterials.2010.01.074.
[51] H. Cao, K. Mchugh, S.Y. Chew, J.M. Anderson, The topographical effect of electrospun nanofibrous scaffolds on the in vivo and in vitro foreign body reaction, J. Biomed. Mater. Res. 93 (2010) 1151–1159, https://doi.org/10.1002/jbm.a.32609.
[52] T.B. Wissing, V. Bonito, E.E. van Haaften, M. van Doeselaar, M.M.C.P. Brugmans, H.M. Janssen, C.V.C. Bouten, A.I.P.M. Smits, Macrophage-driven biomaterial degradation depends on scaffold microarchitecture, Front. Bioeng. Biotechnol. 7 (2019) 87, https://doi.org/10.3389/fbioe.2019.00087.
[53] N.L. Millar, G.A.C. Murrell, I.B. McInnes, Inflammatory mechanisms in tendinopathy – towards translation, Nat. Rev. Rheumatol. 13 (2017) 110–122, https://doi.org/10.1038/nrrheum.2016.213.
[54] P.C.S. Bota, A.M.B. Collie, P. Puolakkainen, R.B. Vernon, E.H. Sage, B.D. Ratner, P.S. Stayton, Biomaterial topography alters healing in vivo and monocyte/macrophage activation in vitro, J. Biomed. Mater. Res. 95 A (2010) 649–657, https://doi.org/10.1002/jbm.a.32893.
[55] B.N. Brown, R. Londono, S. Tottey, L. Zhang, K.A. Kukla, M.T. Wolf, K.A. Daly, J.E. Reing, S.F. Badylak, Macrophage phenotype as a predictor of constructive remodeling following the implantation of biologically derived surgical mesh materials, Acta Biomater. (2012), https://doi.org/10.1016/j.actbio.2011.11.031.
[56] D. Bayik, D. Tross, D.M. Klinman, Factors influencing the differentiation of human monocytic myeloid-derived suppressor cells into inflammatory macrophages, Front. Immunol. 9 (2018) 1–9, https://doi.org/10.3389/fimmu.2018.00608.
[57] C.L. Mendias, J.P. Gumucio, K.I. Bakhurin, E.B. Lynch, S.V. Brooks, Physiological loading of tendons induces scleraxis expression in epitenon fibroblasts, J. Orthop. Res. 30 (2012) 606–612, https://doi.org/10.1002/jor.21550.
[58] J.E. Sero, H.Z. Sailem, R.C. Ardy, H. Almuttaqi, T. Zhang, C. Bakal, Cell shape and the microenvironment regulate nuclear translocation of NF-κB in breast epithelial and tumor cells, Mol. Syst. Biol. 11 (2015) 790, https://doi.org/10.15252/msb.20145644.
[59] B. Chen, C. Co, C.C. Ho, Cell shape dependent regulation of nuclear morphology, Biomaterials 67 (2015) 129–136, https://doi.org/10.1016/j.biomaterials.2015.07.017.
[60] S.A. Wickström, C.M. Niessen, Cell adhesion and mechanics as drivers of tissue organization and differentiation: local cues for large scale organization, Curr. Opin. Cell Biol. 54 (2018) 89–97, https://doi.org/10.1016/j.ceb.2018.05.003.
[61] A. Elosegui-Artola, I. Andreu, A.E.M. Beedle, A. Lezamiz, M. Uroz, A.J. Kosmalska, R. Oria, J.Z. Kechagia, P. Rico-Lastres, A.L. Le Roux, C.M. Shanahan, X. Trepat, D. Navajas, S. Garcia-Manyes, P. Roca-Cusachs, Force triggers YAP nuclear entry by regulating transport across nuclear pores, Cell 171 (2017) 1397–1410, https://doi.org/10.1016/j.cell.2017.10.008 e14.
[62] M. Stolk, F. Klatte-Schulz, A. Schmock, S. Minkwitz, B. Wildemann, M. Seifert, New insights into tenocyte-immune cell interplay in an in vitro model of inflammation, Sci. Rep. (2017), https://doi.org/10.1038/s41598-017-09875-x.
[63] L.A. Ortiz, M. DuTreil, C. Fattman, A.C. Pandey, G. Torres, K. Go, D.G. Phinney, Interleukin 1 receptor antagonist mediates the antiinflammatory and antifibrotic effect of mesenchymal stem cells during lung injury, Proc. Natl. Acad. Sci. Unit. States Am. 104 (2007) 11002–11007, https://doi.org/10.1073/pnas.0704421104.
[64] P. Chomarat, J. Banchereau, J. Davoust, A.K. Palucka, IL-6 switches the differentiation of monocytes from dendritic cells to macrophages, Nat. Immunol. 1 (2000) 510–514 http://www.nature.com/doifinder/10.1038/82763%0Afile:///Files/08/0834F408-6077-45D8-9DB2-022477631918.pdf%0Apapers3://publication/doi/10.1038/82763.
[65] A. Mantovani, A. Sica, S. Sozzani, P. Allavena, A. Vecchi, M. Locati, The chemokine system in diverse forms of macrophage activation and polarization, Trends

Immunol. 25 (2004) 677–686, https://doi.org/10.1016/j.it.2004.09.015.
[66] C.N. Manning, C. Martel, S.E. Sakiyama-Elbert, M.J. Silva, S. Shah, R.H. Gelberman, S. Thomopoulos, Adipose-derived mesenchymal stromal cells modulate tendon fibroblast responses to macrophage-induced inflammation in vitro, Stem Cell Res. Ther. 6 (2015), https://doi.org/10.1186/s13287-015-0059-4 1DUMMY.
[67] B.N. Brown, B.D. Ratner, S.B. Goodman, S. Amar, S.F. Badylak, Macrophage polarization: an opportunity for improved outcomes in biomaterials and regenerative medicine, Biomaterials 33 (2012) 3792–3802, https://doi.org/10.1016/j.biomaterials.2012.02.034.
[68] S. Franz, S. Rammelt, D. Scharnweber, J.C. Simon, Immune responses to implants - a review of the implications for the design of immunomodulatory biomaterials, Biomaterials (2011), https://doi.org/10.1016/j.biomaterials.2011.05.078.
[69] A.C. Abraham, S.A. Shah, M. Golman, L. Song, X. Li, I. Kurtaliaj, M. Akbar, N.L. Millar, Y. Abu-Amer, L.M. Galatz, S. Thomopoulos, Targeting the NF-κB signaling pathway in chronic tendon disease, Sci. Transl. Med. 11 (2019) eaav4319, , https://doi.org/10.1126/scitranslmed.aav4319.
[70] N. Rajan, J. Habermehl, M.F. Coté, C.J. Doillon, D. Mantovani, Preparation of ready-to-use, storable and reconstituted type I collagen from rat tail tendon for tissue engineering applications, Nat. Protoc. 1 (2007) 2753–2758, https://doi.org/10.1038/nprot.2006.430.
[71] K. Phelan, K.M. May, Basic techniques in mammalian cell tissue culture, Curr. Protoc. Cell Biol. 2015 (2015) 1.1.1–1.1.22, https://doi.org/10.1002/0471143030.cb0101s66.
[72] A.D. Schoenenberger, A. Schipanski, V. Malheiro, M. Kucki, J.G. Snedeker, P. Wick, K. Maniura-Weber, Macrophage polarization by titanium dioxide ($TiO_2$) particles: size matters, ACS Biomater. Sci. Eng. 2 (2016) 908–919, https://doi.org/10.1021/acsbiomaterials.6b00006.
[73] S. Tsuchiya, M. Yamabe, Y. Yamaguchi, Y. Kobayashi, T. Konno, K. Tada, Establishment and characterization of a human acute monocytic leukemia-cell line (Thp-1), Int. J. Canc. 26 (1980) 171–176, https://doi.org/10.1002/Ijc.2910260208.
[74] J. Schindelin, I. Arganda-Carreras, E. Frise, V. Kaynig, M. Longair, T. Pietzsch, S. Preibisch, C. Rueden, S. Saalfeld, B. Schmid, J.-Y. Tinevez, D.J. White, V. Hartenstein, K. Eliceiri, P. Tomancak, A. Cardona, Fiji: an open-source platform for biological-image analysis, Nat. Methods 9 (2012) 676, https://doi.org/10.1038/nmeth.2019.